An Approximate Method for Predicting Pressure Distributions on Blunt Bodies at Angle of Attack

ROBERT L. STALLINGS JR.* AND JAMES F. CAMPBELL*
NASA Langley Research Center, Hampton, Va.

An approximate method for predicting pressure distributions in the vertical plane of symmetry on blunt bodies at angle of attack is presented. The method is applied to two families of blunt bodies: 1) spherical cap bodies with rounded shoulders varying from a flat disk to a hemisphere, and 2) large angle cones having apex angles ranging from 120° to 180°. Hand calculations for both families have been made for angles of attack up to 15° and for a freestream Mach number of 4.63. Good agreement is generally shown between experiment and calculated values through the range of variables investigated. Sonic-point and stagnation-point locations are required inputs of the approximate method. An iteration scheme is presented, which adequately predicts the sonic-point locations. Moreover, it was necessary to use experimental stagnation-point locations in the approximate method.

Nomenclature

C_p = pressure coefficient, $(p - p_\infty)/q_\infty$
d = base diameter
K = constant in $\sin^2$ pressure law
M_∞ = freestream Mach number
p, p_∞ = local and freestream static pressure, respectively
$\bar{p}, \bar{p}_*, \bar{p}_{FD}$ = ratio of local pressure to pressure at stagnation point, value of this ratio at sonic point, and values on flat disk, respectively
$\bar{p}_w, \bar{p}_L$ = value of p along windward and leeward rays, respectively
q_∞ = freestream dynamic pressure
r_n, r_c = nose radius and shoulder radius, respectively, of variable nose and shoulder radii bodies
R = base radius
s, s_{stag}, s_*, s_2 = distance measured along body surface from axis of symmetry, value to stagnation point, value to sonic point, and value to juncture of body nose and base
V_∞ = freestream velocity
α = angle of attack
θ = complement of surface slope at shoulder of spherical cap bodies
δ, δ_* = complement of angle through which flow has expanded on body surface relative to stagnation point, value at sonic point
δ_c = half angle of cone
ϵ, ϵ_0 = nose radius and maximum nose radius, respectively, of spherically blunted cone for given δ_c, the radius being tangent to the cone surface
ϕ = meridian angle
λ = exponent in equation for $\bar{p}_{FD}$, see Eq. (4)

Introduction

FOR entry into low-density planetary atmospheres, body shapes with low-ballistic coefficients (large-angle cones, flat disks, spherical caps, and spherical caps with various degrees of corner rounding) are of interest. Many reports contain experimental data and theoretical methods for defining the flowfields on such bodies (e.g., Refs. 1–14). However, most of the theoretical methods are restricted to zero angle of attack. Reliable estimates of the pressure distributions for a wide variety of smoothly contoured blunt bodies at zero angle of attack can be obtained from a simplified method recently published by Love[1] and referred to as "the $\sin^2$ deficiency method." This method gives results that are comparable to those achieved by lengthy numerical procedures. This paper presents an extension of the method to the case of angle of attack. For the angle-of-attack case heretofore, the only theoretical methods available for confidently predicting pressure distributions for the complete range of blunt bodies under consideration have been numerical schemes requiring machine programing. The present method has been evaluated for two families of blunt bodies: 1) spherical cap bodies with rounded shoulders varying from a flat disk to a hemisphere, and 2) large angle cones having apex angles ranging from 120° to 180°. All results in the form of pressure distributions are present at a freestream Mach number at 4.63 and for angles of attack up to 15°.

Presented as Paper 70-208 at the AIAA 8th Aerospace Sciences Meeting, New York, January 19–21, 1970; submitted February 27, 1970; revision received August 7, 1970.

* Aerospace Engineer. Member AIAA.

Discussion

Love's Method, $\alpha = 0°$

The $\sin^2$ deficiency method as developed by Love[1] accounts for deficiencies in the $\sin^2$ law

$$C_p = K \sin^2\delta \tag{1}$$

that occur for certain blunt bodies; one case being the blunt noses of bodies of revolution approaching the shape of a flat disk. Basically, the method was developed by defining the deficiency of the $\sin^2$ law for a fundamental blunt shape (flat disk) and applying it to various blunt shapes by an approximation routine. The resulting equation for nondimensional pressures between the stagnation point and sonic point of smoothly contoured blunt bodies is

$$\bar{p} = \sin^2\delta - (1 - \bar{p}_{FD})(\sin^2\delta - \bar{p}_*)/(1 - \bar{p}_*) \tag{2}$$

where $\bar{p}_{FD}$ corresponds to pressure on the flat disk at equivalent values of s/s_*. Love found by a variable streamtube approximation that the following equation could be obtained for the pressure distribution on the flat disk

$$\bar{p}_{FD} = 1 - e^{-\lambda}(1 - \bar{p}_*) \tag{3}$$

where

$$\lambda = 4[\ln(s_*/s)]^{1/2} \tag{4}$$

Therefore, if the sonic-point location on a smoothly contoured blunt body is known, Eqs. (2–4) can be used to predict the pressure distribution up to the sonic point. Shown in Fig. 1 are comparisons between calculated and experimental pressure distributions from Ref. 6 for spherical cap bodies with

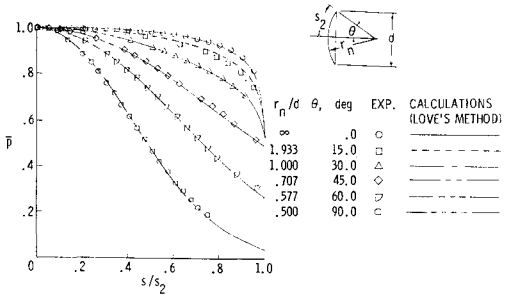

Fig. 1 Comparison between experimental and calculated pressure distributions on spherical cap bodies; $M_\infty = 4.63$, $\alpha = 0°$.

zero corner radius ranging from a flat disk to a hemisphere. Although the calculated distributions shown in Fig. 1 are based on experimentally determined sonic-point locations, these locations for the spherical cap bodies can be adequately predicted by existing methods (e.g., modified Newtonian theory). In general, good agreement is shown between the calculated values and the experimental data up to the sonic point for all models. For those models having $r_n/d \geq 1.0$, the sonic points were located at $s/s_2 = 1.0$ and, therefore, subsonic flow occurred over the entire nose. For the models with $r_n/d \leq 0.707$, both subsonic and supersonic flow occurred over the nose. In the supersonic region, the pressure distributions were calculated as suggested in Ref. 1 by assuming a $\sin^2$ law variation from the sonic point to a match point where the $\sin^2$ law is matched to the Prandtl-Meyer approximation; the Prandtl-Meyer approximation is then used to $s/s_2 = 1.0$. The results of these combined calculations as shown in Fig. 1 ($r_n/d \leq 0.707$) are in good agreement with the experimental data. Results from the combined calculations are further compared with experimental results[6] in Fig. 2 for a group of spherical cap bodies with rounded shoulders. Good agreement is generally shown between calculated and experimental results. Some disagreement does occur, however, in the region between the point of tangency of the nose and shoulder radii and the sonic-point location for the larger values of r_n/d. Within this region, less expansion than indicated by experiment is predicted.

The experimental sonic-point locations[6] which were used for the pressure calculations shown in Fig. 2 are compared with calculated values in Fig. 3. For $r_c/d > 0$, the calculations are based on the method of Ref. 1; and for the spherical cap bodies, $r_c/d = 0$, the calculations are based on modified Newtonian theory. The sonic-point locations for the spherical cap bodies were assumed to be at the sharp corners ($s/s_2 = 1$) if the values of δ at the corners were greater than the value of δ at the sonic point of a hemisphere. The method of Ref. 1 is an iteration scheme where one initially assumes the sonic point is at a location predicted by modified Newtonian theory. By use of this sonic-point location and the flat-disk solution, Eq. (3), a value of $\bar{p}_{FD}$ is calculated at the tangency point of the nose and shoulder radii. This value of $\bar{p}_{FD}$ is interpreted as the value of an effective δ at the tangency point, and the sonic point is then shifted on the body such that the change in surface slope corresponds to the angular differences between the effective δ and the actual δ at the tangency point. Using the new sonic-point location, a new effective δ is calculated, and the process is repeated until negligible changes in sonic-point locations are obtained. As shown in Fig. 3, the calculated values for $r_c/d > 0$ are generally in good agreement with the experimental results. The calculated sonic-point locations for the spherical cap bodies ($r_c/d = 0$) are at the sharp corners for $r_n/d \geq 1.00$. For $r_n/d = 0.707$ calculations indicate the sonic point has moved slightly upstream of the corner, whereas the experimental results indicate $s_*/s_2 \approx 0.90$. Although not shown in Fig. 3, better agreement between calculated and experimental sonic-

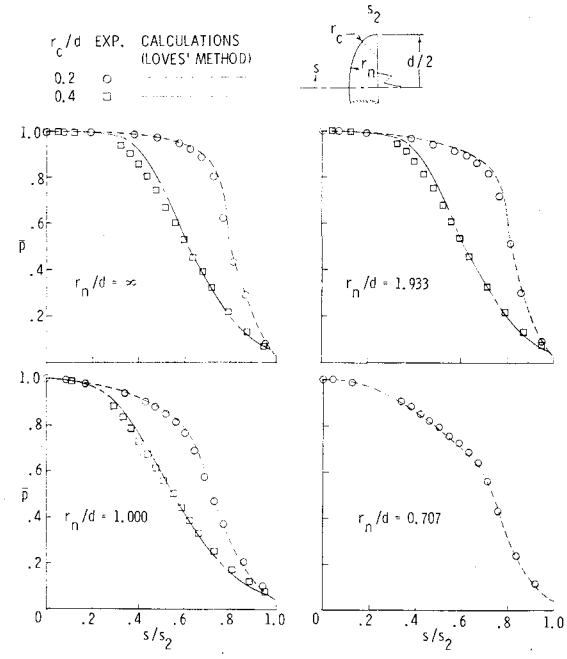

Fig. 2 Comparison between experimental and calculated pressure distributions on bodies with rounded shoulders; $M_\infty = 4.63$, $\alpha = 0°$.

point locations on the spherical cap bodies were obtained for values of $r_n/d < 0.707$.

The $\sin^2$ deficiency method was also applied by Love[1] to cones with half angles exceeding that for sonic flow. The resulting form of Eq. (2) including modifications that adapt it to large angle cones is as follows:

$$\bar{p} = \sin^2\delta - (1 - \bar{p}_{FD})\left(\frac{\sin^2\delta - \bar{p}_*}{1 - \bar{p}_*}\right) + \left(1 - \frac{\epsilon}{\epsilon_0}\right)\left\{(1 - \sin^2\delta)\left(1 - \frac{s}{s_*}\right) + \frac{s/s_*}{2}\left[\bar{p}_{FD} - 1 + \frac{s}{s_*}(1 - \sin^2\delta) + (1 - \bar{p}_{FD})\left(\frac{\sin^2\delta - \bar{p}_*}{1 - \bar{p}_*}\right)\right]\right\} \quad (5)$$

For this family of bodies, the sonic point would, of course, always be located at the sharp shoulder. Comparison of results from Eq. (5) with experimental data from several large angle cones[8,9] is shown in Fig. 4.

Present Method, $\alpha > 0°$

If we can identify the stagnation-point and sonic-point locations for the angle-of-attack case as well as the corresponding values of $\bar{p}_{FD}$, then we should be able to use either Eq. (2) or (5), depending on the shape of body under consideration, to calculate the pressure in the vertical plane of sym-

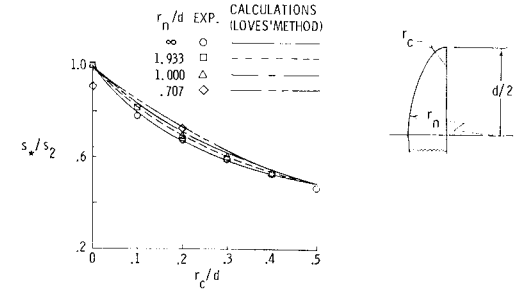

Fig. 3 Comparison between experimental and calculated sonic-point locations on spherical cap bodies with rounded shoulders; $M_\infty = 4.63$, $\alpha = 0°$.

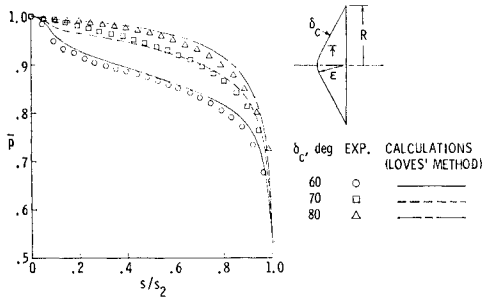

Fig. 4 Comparison of calculated and experimental pressure distributions on large angle cones; $M_\infty = 4.63$, $\alpha = 0°$, $\epsilon/R = 0.25$.

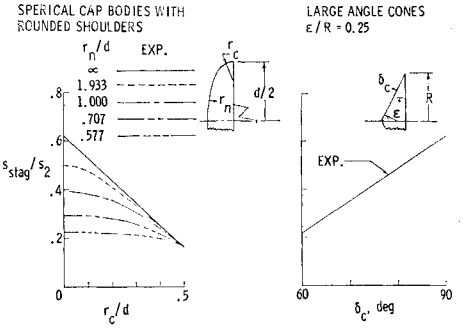

Fig. 6 Measured stagnation-point locations; $M_\infty = 4.63$, $\alpha = 15°$.

metry of a body a tangle of attack by treating the windward meridian and leeward meridian as separate bodies. The respective surface locations on these bodies, relative to the stagnation point and nondimensionalized by the distance from the stagnation point to the sonic point, would be related to the corresponding flat disk locations similar to the method used for $\alpha = 0°$. The key to the application of the $\sin^2$ deficiency method to the angle-of-attack case is, therefore, the definition of the sonic-point and stagnation-point locations and the values of $\bar{p}_{FD}$ for angle of attack.

Sonic-point locations for the large angle cones were always at the sharp shoulders for the ranges of cone angle ($60° \leq \delta_c \leq 90°$) and angles of attack ($\alpha \leq 15°$) investigated. For the spherical cap bodies with rounded shoulders at angle of attack, the sonic-point locations were approximated by assuming the sonic points shifted on the body to such locations that the change in surface slope corresponded to the change in angle of attack. With increasing angle of attack, the sonic point on the windward side of the body would move away from the axis of symmetry, whereas on the leeward side it would move toward the axis of symmetry. A comparison of sonic-point locations calculated by this method with locations determined from experimental pressure distributions from Ref. 7 is shown in Fig. 5. In general, good agreement is shown between calculated and experimental values.

Stagnation-point locations for the spherical cap bodies with rounded shoulder and the large angle cones determined from the experimental pressure distributions of Refs. 7, 8, and 9 are shown in Fig. 6 at $\alpha = 15°$. Although no satisfactory simplified method was developed for predicting these stagnation-point locations, the results shown in Fig. 6 can be extended to a wide range of freestream conditions for any body of the general shapes shown. As discussed in Refs. 7, 8, and 9, the pressure distributions for these bodies at $M_\infty = 4.63$ were essentially invariant with Mach number and, in fact, the pressure distributions obtained at this Mach number were almost the same as results in the literature on similar bodies for Mach numbers up to 10. The results shown in Fig. 6 should, therefore, be applicable for Mach numbers much greater than 4.63. For angles of attack between 0° and 15°, a linear variation of s_{stag}/s_2 with α was found to satisfactorily approximate the measured locations. This approximation should not be extended, however, to angles of attack greater than 15°.

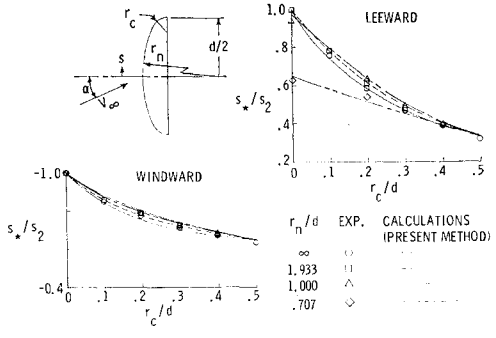

Fig. 5 Comparison between experimental and calculated sonic-point locations on spherical cap bodies with rounded shoulders; $M_\infty = 4.63$, $\alpha = 15°$.

Having defined the sonic-point and stagnation-point locations for the classes of bodies under consideration, the only remaining input for the angle-of-attack extension of Love's method is an expression for the pressure distribution on the flat disk at angle of attack. In order to determine if Eq. (3) could be applied by treating the windward and leeward meridians of the flat disk as two separate bodies, the experimental pressure distributions of Ref. 8 at angles of attack up to 15° were plotted as shown in Fig. 7a. If Eq. (3) were applicable, the results shown would have collapsed into a single curve defined by Eq. (3) for both the windward and leeward sides. This correlation apparently occurs on the windward side of the flat disk. The pressure distributions on the leeward side form a family of unique curves for the range of angle of attack shown. The variation of the measured leeward distributions with angle of attack suggests an equation of the following form:

$$\bar{p}_{FD} = 1 - e^{-f(\alpha)\lambda}(1 - \bar{p}_*) \tag{6}$$

The following expression for $f(\alpha)$ was found to result in the best agreement with experimental distributions

$$f(\alpha) = 1.0 - 0.02125\alpha \tag{7}$$

where α is in degrees.

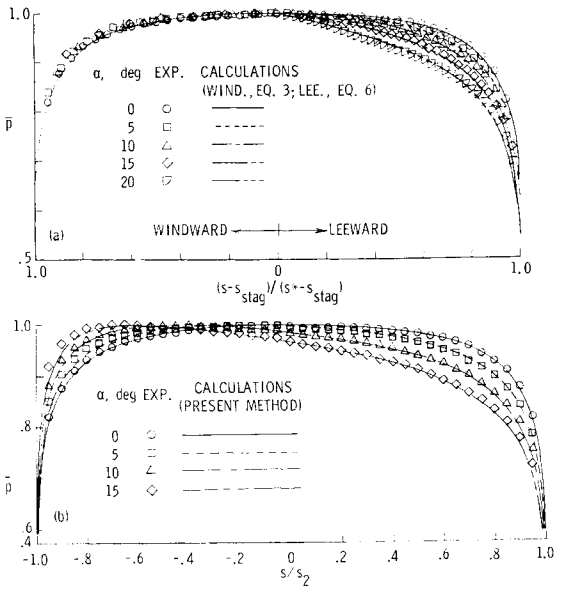

Fig. 7 Comparison between experimental and calculated pressure distributions on flat disk; $M_\infty = 4.63$.

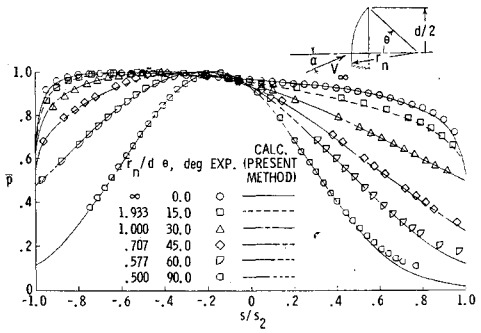

Fig. 8 Comparison between calculated and experimental pressure distributions on spherical cap bodies; $M_\infty = 4.63$, $\alpha = 15°$.

The agreement shown in Fig. 7a between calculations and experiment, where Eq. (3) is used windward of the stagnation point and Eqs. (6) and (7) are used leeward of the stagnation point, is considered adequate for this study. The results shown in Fig. 7a are replotted in Fig. 7b, showing the comparison between calculations and experiment with the coordinate s/s_2 expressed in its usual form.

Preliminary calculations of pressure distributions for both families of bodies at angle of attack indicated that better agreement with experimental data could be obtained in the vicinity of the sonic region by using a new angle δ', defined as

$$\delta' = \delta \pm \Delta\delta \left[(s/s_2 - s_{stag}/s_2)/(s*/s_2 - s_{stag}/s_2)\right] \quad (8)$$

for

$$s/s_2 \leq s*/s_2$$

and where $\Delta\delta$ is the angle between the freestream velocity vector and the surface normal at the stagnation point. The + and − signs on the right-hand side of Eq. (8) correspond to leeward and windward of the stagnation point, respectively.

Having defined procedures for evaluating the required inputs to the present method, pressure distributions were calculated for the spherical cap bodies with rounded shoulders and the large angle cones at angles of attack. For the two families of bodies under consideration, Eq. (2) or (5) together with Eqs. (6) and (8) were used with sonic-point and stagnation-point locations determined either by experiment or calculation. Pressure distributions in the supersonic region were calculated the same as for $\alpha = 0°$ using the standard form of δ.

Shown in Fig. 8 is a comparison of the calculated and experimental pressure distributions[7] for the spherical cap bodies at $\alpha = 15°$. The calculations within the leeward subsonic region for all bodies, with the exception of the flat disk, are actually based on $\bar{p}_{FD}$ values for $\alpha = 0°$ rather than values evaluated from Eq. (6) for the respective angles of attack. Use of $\bar{p}_{FD}$ values from Eq. (6) for the leeward side of the bodies, with the exception of the flat disk, resulted in pressures below the experimental values. Equation (6) was used, however, for calculating the windward pressure distributions. Comparison of calculated and experimental pressure distributions for the spherical cap bodies with rounded shoulders at $\alpha = 15°$ are shown in Fig. 9. Similar to the comparison shown for $\alpha = 0°$, Fig. 2, the calculated values slightly overpredict the measured values between the point of tangency of the nose and shoulder radii and the sonic point, however, the agreement is somewhat better for the $\alpha = 15°$ case.

Shown in Fig. 10 is a comparison of calculated and experimental pressure distributions[8,9] for the large angle cones. Windward of the stagnation point for both angles of attack, good agreement is shown between experiment and calculations. Leeward of the stagnation point at $\alpha = 5°$, the experimental pressures are adequately predicted by calculations with the exception of the region near the juncture of the spherical segment nose and cone frustum of the 60° cone.

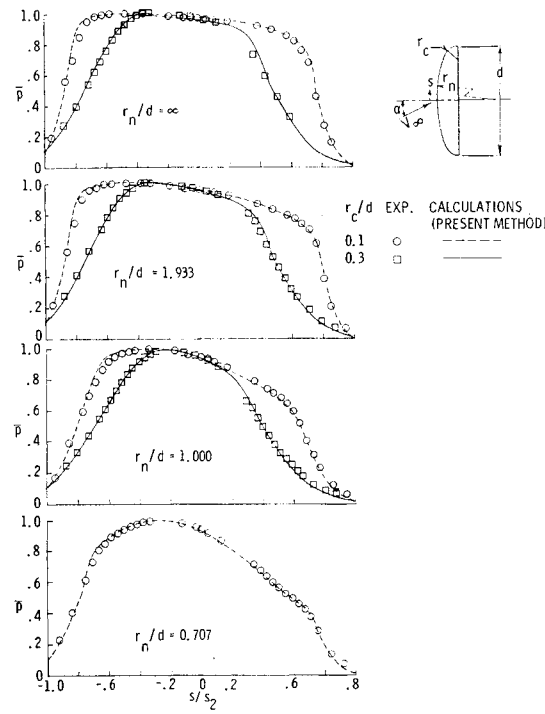

Fig. 9 Comparison between experimental and calculated pressure distributions on spherical cap bodies with rounded shoulders; $M_\infty = 4.63$, $\alpha = 15°$.

Within this region, the flow expands more rapidly than predicted. The extent of disagreement within this region increases with increasing angle of attack to 15° and also apparently extends to the larger angle cones. The measured pressures on the leeward conical surface of the 60° cone at $\alpha = 15°$ are significantly overpredicted by the calculations. This disagreement is believed to result from the fact that the tangent cone for this surface at this angle of attack would have an attached shock wave. Although not indicated on the figure, the local static pressure for this tangent cone is approximately the same as that measured within the region of constant pressure on the leeward 60° cone surface at $\alpha = 15°$.

Force and moment coefficients determined by integration of the calculated pressure distributions were, as shown in Ref. 15, in good agreement with force balance measurements for both families of bodies.

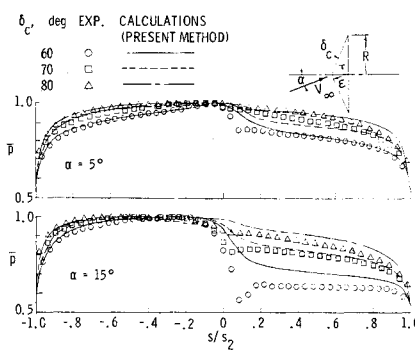

Fig. 10 Comparison between experimental and calculated pressure distributions on large angle cones; $M_\infty = 4.63$, $\epsilon/R = 0.25$.

Concluding Remarks

An approximate method for predicting pressure distributions in the vertical plane of symmetry on blunt bodies at angle of attack is presented. The method is applied to two families of blunt bodies: 1) spherical cap bodies with rounded shoulders, and 2) large angle cones. Pressure distributions calculated from this "extended $\sin^2$ deficiency method" are in good agreement with experiment through most of the range of geometrical variables investigated.

References

[1] Love, E. S. et al., "Some Topics in Hypersonic Body Shaping," AIAA Paper 69-181, New York, 1969.

[2] South, J. C., "Calculation of Axisymmetric Supersonic Flow Past Blunt Bodies with Sonic Corners, Including a Program Description and Listing," TN D-4563, 1968, NASA.

[3] Kaattari, G. E., "A Method for Predicting Shock Shapes and Pressure Distributions for a Wide Variety of Blunt Bodies at Zero Angle of Attack," TN D-4539, 1968, NASA.

[4] Van Dyke, M. D. and Gordon, H. D., "Supersonic Flow Past a Family of Blunt Axisymmetric Bodies," TR R-1, 1959, NASA.

[5] Belotserkovskii, O. M., "Flow With a Detached Shock Wave about a Symmetric Profile," *Journal of Applied Mathematics and Mechanics*, Vol. 22, No. 2, 1958, pp. 279–296.

[6] Stallings, R. L., Jr., "Experimentally Determined Local Flow Properties and Drag Coefficients for a Family of Blunt Bodies at Mach Numbers From 2.49 to 4.63," TR R-274, 1967, NASA.

[7] Stallings, R. L., Jr. and Howell, D. T., "Experimental Pressure Distributions for a Family of Blunt Bodies at Mach Numbers From 2.49 to 4.63 and Angles of Attack From 0° to 15°," TN D-5392, 1969, NASA.

[8] Campbell, J. F. and Tudor, D. H., "Pressure Distributions on 140°, 160°, and 180° Cones at Mach Numbers From 2.30 to 4.63 and Angles of Attack From 0° to 20°," TN D-5204, 1969, NASA.

[9] Stallings, R. L., Jr. and Tudor, D. H., "Experimental Pressure Distributions on a 120° Cone at Mach Numbers From 2.96 to 4.63 and Angles of Attack From 0° to 20°," TN D-5054, 1969, NASA.

[10] Ashby, G. C., Jr. and Goldberg, T. J., "Application of Generalized Newtonian Theory to Three-Dimensional Sharp-Nose Shock-Detached Bodies at Mach 6 for Angles of Attack up to 25°," TN D-2550, 1965, NASA.

[11] Trimmer, L. L., "Study of the Blunt Body Stagnation Point Velocity Gradient in Hypersonic Flow," TR-6899, AD 669378, May 1968, Arnold Engineering Development Center, Tullahoma, Tenn.

[12] Traugott, S. C., "An Appropriate Solution of the Direct Supersonic Blunt-Body Problem for Arbitrary Axisymmetric Shapes," *Journal of the Aerospace Sciences*, Vol. 27, No. 5, May 1960, pp. 361–370.

[13] Boison, J. C. and Curtiss, H. A., "An Experimental Investigation of Blunt Body Stagnation Point Velocity Gradient," *ARS Journal*, Vol. 29, No. 2, Feb. 1959, pp. 130–135.

[14] Lawson, W. A., McDearman, R. W., and Rainey, R. W., "Investigation of the Pressure Distributions on Reentry Nose Shapes at a Mach Number of 3.55," TM X-244, 1960, NASA.

[15] Stallings, R. L., Jr. and Campbell, J. F., "An Approximate Method for Predicting Pressure Distributions on Blunt Bodies at Angle of Attack," AIAA Paper 70-208, New York, 1970.